The Science and Challenges for Future Detector Development in High Energy Physics

James E. Brau
University of Oregon, Eugene, OR 97403-1274, USA

The compelling scientific goals of future high energy physics experiments demand significant advances in detector technology. Particle physics opportunities have never been so bright, but the detector challenges must be met. With the underlying mechanism for electroweak symmetry breaking, the mass hierarchy problem, new forms of matter and forces such as those of supersymmetrry, extra dimensions, discovery of the meaning of dark matter and dark energy, or deeper understanding of structure of the neutrino sector all being realistic targets, detector development efforts are strongly motivated. Advances for future experiments can be anticipated, based on past trends, including developments in microelectronics, materials technology, and radiation tolerance. Several examples of developments for future experiments at the Super Large Hadron Collider, the International Linear Collider, the Super B Factory, and neutrino experiments are outlined.

1. INTRODUCTION

Future high energy physics detectors will be challenged by scientific questions of great significance, and unprecedented operating conditions. Successfully confronting these challenges will lead to powerful new insights into the nature of the universe.

These challenges will include the Super Large Hadron Collider upgrades, with high radiation levels, pileup, and backgrounds. The International Linear Collider will require precision measurements that will press detector performance. The Super B Factory aims for 10^{36} $cm^{-2}sec^{-1}$ luminosity, introducing many challenges not faced at the current B factories. Neutrino detectors require massive volumes, with highly efficient detection. Rare kaon decay and τ/charm detectors will demand high bandwidth and high precision. Many other experiments need detector advances for important efforts critical to advances in high energy physics, such as dark matter detectors, or space-based experiments. The challenges for these associated projects will be introduced in a later talk at this conference.[1]

This paper concentrates on accelerator based high energy physics experiments. The author has attempted to create a broad and general overview, but by necessity, this treatment is selective. All important work could not be included within the constraints.

2. PHYSICS GOALS FOR THE COMING EXPERIMENTS

The Standard Model is a well tested, precise description of what has been measured. But there is certainty that it is not a complete theory. In order to make progress in theory now, advances are needed on a variety of experimental fronts:

- electroweak symmetry breaking and the origin of mass
- the hierarchy problem
- dark matter (dark energy)
- neutrino mass
- the matter/anti-matter asymmetry
- unification of gravity (and the connection to extra dimensions?)

Experiment must now lead the way to understanding on these topics and others. Detector R&D is critical to advance our capabilities for upgraded and new experiments. The compelling physics questions demand ever improved detector capabilities. Furthermore, accelerator technology is advancing significantly, providing excellent opportunities, and increasing the demands on detectors.

2.1. Electroweak Symmetry Breaking

The mechanism of electroweak symmetry breaking is one of the key fundamental unknowns of particle physics today. The Standard Model provides a good description of all experimental data. An example is shown in Figure 1, where the cross section for W pair production measured at LEP is compared to the Standard Model expectations.[2] Excellent agreement is found. The neutrino exchange component alone far exceeds the measurements, while the full Standard Model description aligns with the data.

Figure 2 presents the constraint on the mass of the Standard Model Higgs boson derived from the electroweak precision measurements. In the context of the Standard Model, these measurements indicate the mass of the Standard Model Higgs boson is less than about 166 GeV with 95 percent confidence.[3] This limit increases to 199 GeV when including the LEP-2 direct search limit of 114 GeV, shown by the low mass shading of Figure 2. Discovery of a Standard Model-like Higgs boson is therefore anticipated at the Tevatron or the LHC. In the absence of a Standard Model-like Higgs boson signal, we can expect insight into the alternative mechanisms, such as those involving new strong interactions, extra dimensions,

or other explanation. Whether a Standard Model-like Higgs boson is discovered, or not, follow-up experiments such as those being prepared for the ILC, will lead to deeper understanding. Detector R&D is needed to ensure such experiments fully exploit the opportunity.

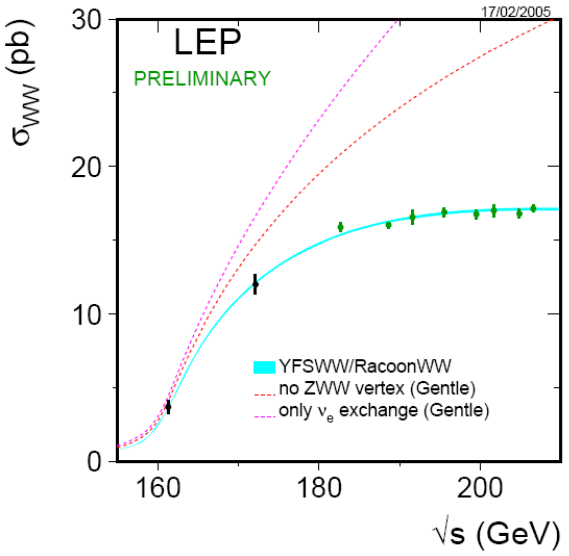

Figure 1. Cross section for W pair production in electron-positron collisions at LEP. [2]

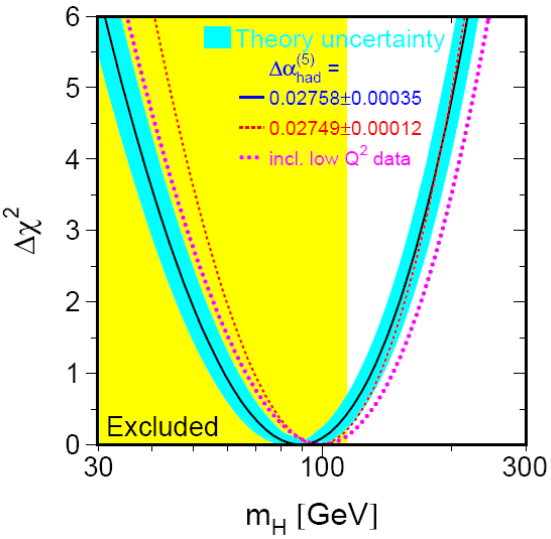

Figure 2. . The $\Delta\chi^2$ curve derived from high-Q^2 precision electroweak measurements, performed at LEP and by SLD, CDF, and D0, as a function of the Higgs-boson mass, assuming the Standard Model to be the correct theory of nature. [3]

2.2. Supersymmetry

Supersymmetry is a popular notion, motivated by methods to deal with the hierarchy problem, and inspired by string theory. Discovery would reveal a new form of matter, and would initiate a new era of particle physics, with numerous states to discover and investigate. The reach of the LHC could provide the discovery, which would need to be followed by new experiments, probing the details of the new states.

2.3. Rare Decays

Studies of rare decays of particles continues to be an important tool for investigation, providing a window to the higher mass scales. Such experiments should include decays of the B mesons, the charmed mesons, the K mesons, the tau lepton, and the muon. For example, the current understanding[4] of CP violation is limited by experimental sensitivity achieved in the B Factories (see Figure 3).

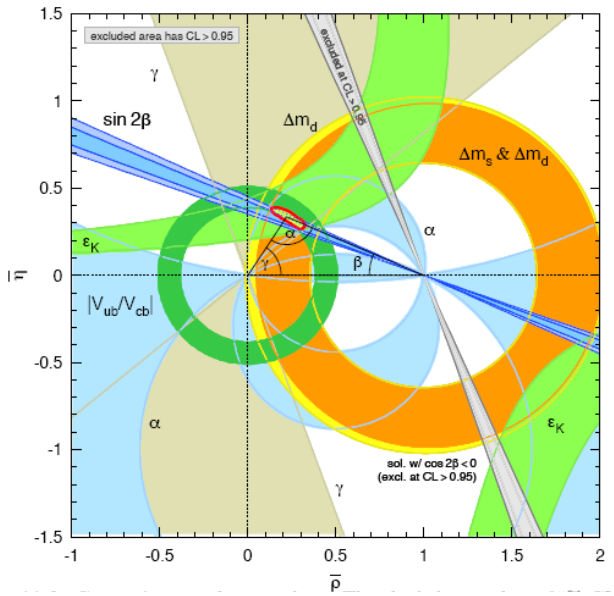

Figure 3. Constraints on the ρ, η plane. Shaded areas have 95% CL. [4]

2.4. Neutrinos

The past decade was exciting on the neutrino front, with neutrino mass established. Experiments are preparing to explore the mixing angles, the neutrino mass ordering, and the neutrino mass scale with new levels of sensitivity. Figure 4 presents the current status of measurements.[5]

Neutrino-less double beta decay experiments provide a means to reach electron neutrino mass sensitivities of a few tens of milli-eV, in a few years.

2.5. Astrophysics Connections

Particle physics is coupled to many issues in astrophysics today. These topics will be covered by the next speaker.[1]

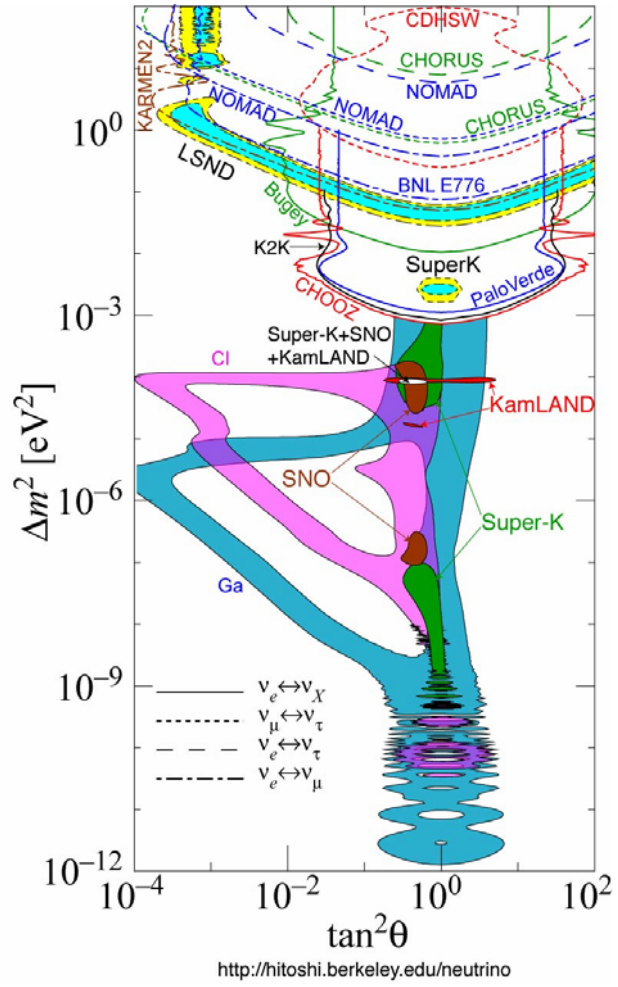

Figure 4. 90% CL allowed regions for the neutrino oscillation parameters Δm^2 and $\tan^2\theta$.[5]

3. EXPERIMENTAL OPPORTUNITIES AND DETECTOR CHALLENGES

With the many fundamental issues within experimental reach for the current and future experiments, we enter an interesting era for particle physics. This paper addresses the detector challenges for the future experiments, such as those at the upgraded LHC (Super LHC), the International Linear Collider, the Super B Factory, and the new neutrino facilities.

3.1. Super LHC

Following the initial period of operation at the design luminosity of 10^{34} cm^{-2} sec^{-1}, ATLAS and CMS could extend their physics reach with upgrades for Super LHC, capable of operations at 10^{35} cm^{-2} sec^{-1}. This would stretch the physics reach significantly. Figure 6 and Figure 6 illustrate this physics extension for two of the physics topics.[6,7]

The discovery reach for supersymmetry would increase by about 20-30%, with access to rare decays of the Higgs, or flavor changing neutral currents through top decays. Important precision measurements become accessible, including Higgs-to-fermion/boson couplings, Higgs self-coupling (perhaps), triple gauge couplings, quartic gauge couplings, strong VL-VL scattering, and SUSY mass measurements.

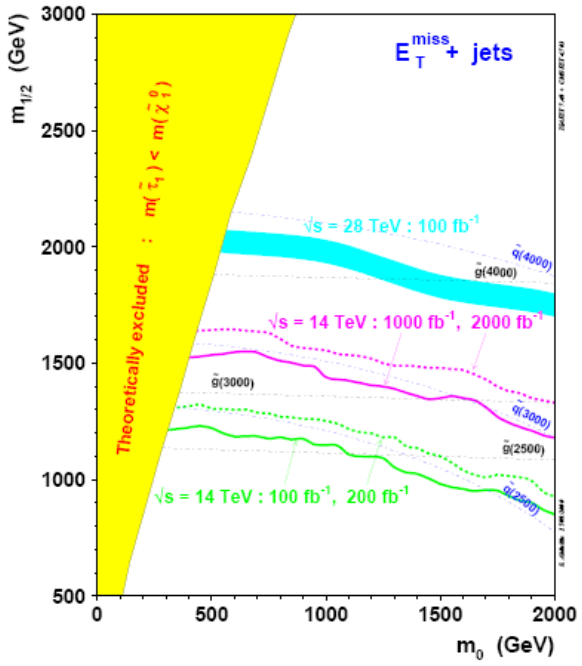

Figure 5. Expected 5σ discovery contours in the mSUGRA plane m_0 versus $m_{1/2}$ for $A_0 = 0$, tanβ=10 and μ < 0. The various curves show the potential of the CMS experiment at the standard LHC (for luminosities of 100 fb^{-1}and 200 fb^{-1}), at the SLHC (for 1000 f^{-1} and 2000 fb^{-1}), and (for comparison) at a machine with a centre-of-mass energy of 28 TeV. [6]

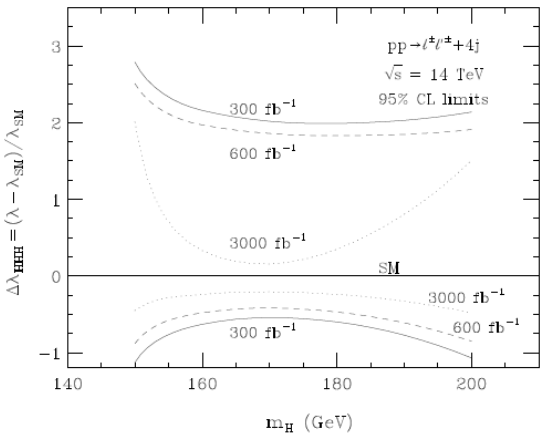

Figure 6. Limits achievable at 95% CL for $\_\lambda_{HHH} = (\lambda - \lambda_{SM})/\lambda_{SM}$ in $pp \to \ell^\pm\ell'^\pm + 4j$ at the LHC. [7]

The LHC experiments are planning to fully exploit the Super LHC opportunity by upgrading the detectors to achieve performance at the higher luminosity similar to that at the LHC.[8] This will require improved tracking, modifications to the triggers and data acquisition, and attention to other experimental issues, such as the forward crystals in CMS.

The tracking is particularly degraded by the intense levels of radiation in the detector. Fluences of $>10^{16}$ /cm^2 @ 5 cm (~400 MRad), $> 10^{15}$ /cm^2 @ 20 cm (~40 MRad), and $> 2 \times 10^{14}$ /cm^2 @ 50 cm (~10 MR) are anticipated in the central detector. The technology choice for tracking elements is dictated by this environment.

Pileup is another issue which must be addressed, with 200 interactions per crossing expected, and a central rapidity density of 1500 tracks per unit of pseudorapidity.[9] This means nearly 10,000 charge tracks within $|\eta| < 3$ per crossing! (The rate could be reduced if the bunch spacing is reduced.) The geometry of the tracker is fundamentally dictated by the pileup rate.

A third consequence of the high radiation environment is the concentration of radiation in the forward endcaps, a serious issue for the forward crystals in CMS.

Tracking considerations have led to a number of preliminary conclusions. Silicon microstrips should work outside a 60 cm radius. Six layers with pitches of 80-160 μm will preserve the LHC performance. Due to the large area covered, it will be very important to exploit 12 inch wafer technology. The fluences would be twice as large as those tested for LHC. Conventional pixels should function outside a 20 cm radius. The pixel cells should be about ten times larger than current LHC pixels, but ten times smaller than current silicon microstrips.

Inside a 20 cm radius, a new technology is required. None currently developed can provide a viable solution. Pixel sizes should be of the order of 50 μm x 50 μm. Concepts being studied include CVD diamond, monolithic pixels, and cryogenic silicon

The RD50 Collaboration has a large, coordinated effort underway to address these issues. With 50 institutes, and 250 individuals, solutions involve solving a number of technical issue, including the depletion voltage changes incurred by silicon devices, motivating investigations of Czochralski silicon and oxygenated p-type silicon. Fluences above 10^{15} /cm^2 force efforts beyond materials engineering into entirely new concepts, such as thin/epitaxial silicon detectors or 3D detectors.

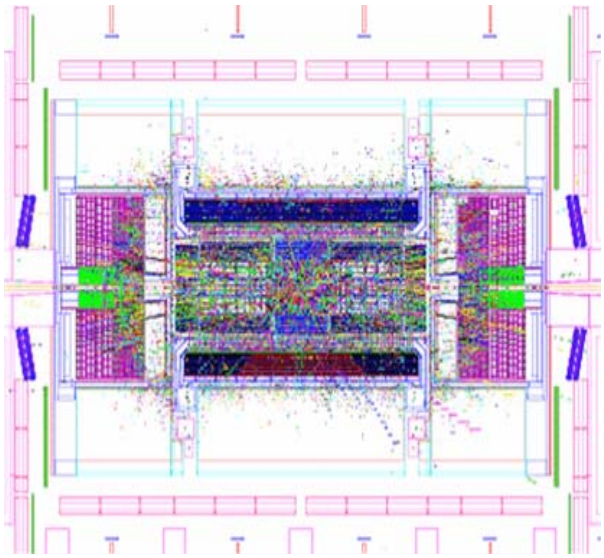

Figure 7. Illustration of pile-up in the ATLAS detector at the Super LHC, showing ~10,000 particle within $|\eta| < 3.2$. [9]

3.2. ILC

The International Linear Collider (ILC) presents challenges of a different nature from those of the LHC. The ILC physics places a premium on precision jet measurements and flavor tagging, in an environment where full event reconstruction is possible. Examples of important channels involving multijets are tth (8 jets), hZ (4 jets), and hhZ (6 jets). Full reconstruction of these final states will be important, and should be feasible, but achieving good efficiency is critical. Supersymmetric signatures depend on this. Lepton identification, τ reconstruction, and quark flavor tagging are all valuable signatures. Given the environment, very precise vertex reconstruction is possible, complementing the calorimetry. Precision tracking is required for decay-mode independent Higgs detection through the Higgstrahlung reaction:

$$e\,e \rightarrow Z\,H$$
$$Z \rightarrow l^+l^-$$
$$H \rightarrow \text{anything}$$

Flavor tagging at the ILC is a critical requirement for the physics goals, such as testing the Standard Model character of the Higgs branching fractions.

Figure 8 illustrates the deviation from Standard Model for several Higgs boson decays modes and the expected ILC sensitivity for the MSSM.[10] This capability will be provided by a billion element pixel vertex detector, with ~3 micron point resolution. The goal is to restrict each layer of the vertex detector to 0.1% X_0. The SLD vertex detector, comprising 307 million pixels, maintained a better than 4 micron point resolution over the entire system.[11]

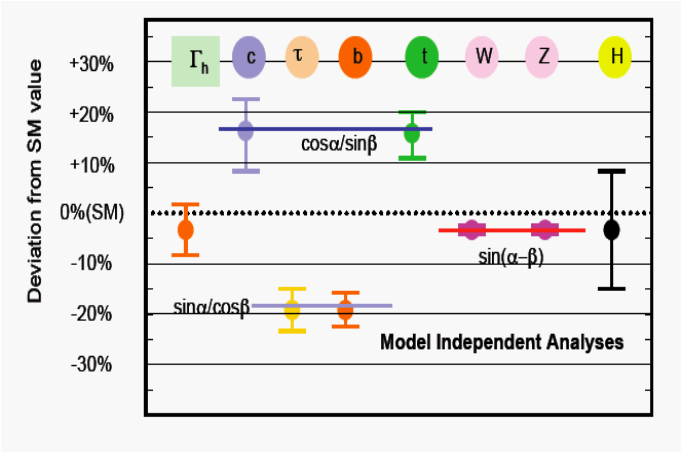

Figure 8. Deviation from Standard Model values for the Higgs couplings in the 2 Higgs doublet model.[10]

3.3. Super B Factory

The Super B Factory has potential for significant improvement in the precision of B physics measurements, and the consequential advanced testing of the unitarity triangle. Many of the useful channels have been studied,[12] demonstrating that many sensitivities are superior to LHC-b, thereby complementing the hadron collider.

While these measurements are feasible, the B Factory rates, backgrounds, occupancies, and radiation doses are challenging. An extrapolation of BaBar experience[13] shows for 10^{36} cm^{-2} sec^{-1}, Silicon Vertex Tracker exposures of 7 MRad/year, 100% occupancy in the Drift Chamber, and more than 10 hits/crystal/event in the Electromagnetic Calorimeter. For a Linear Super B Factory, there is a thousand-fold reduction in beam currents seen by the detector, significantly relaxing these issues.

3.4. Neutrinos

Neutrino physics has been very productive in recent years, motivating increased sensitivity in search of the yet unmeasured parameters: the neutrino mass ordering, the neutrino mass scale, the third mixing angle θ_{13}, and the CP phase δ. Accelerator-based experiments demand ever more massive, more sensitive detectors to achieve sensitivity.

Figure 9 illustrates the possibilities for progress in discovery reach for the third mixing angle.[14] Included in this picture of the possible evolution are the reactor-based experiments, which offer an alternative capability.

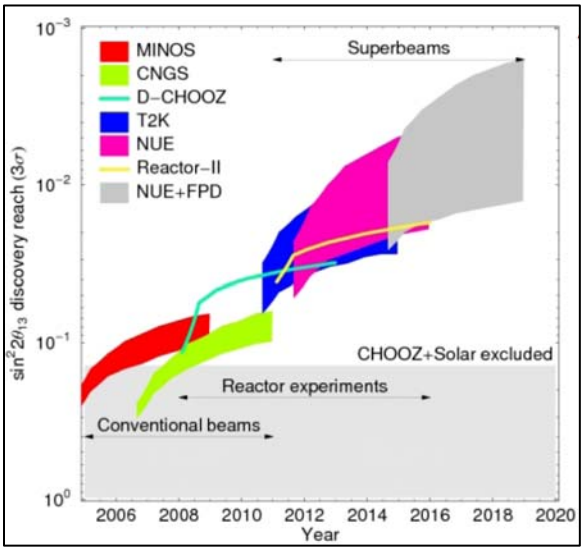

Figure 9. Discovery reach for anticipated future neutrino experiments.[14]

The neutrino mass scale may be reached through neutrino-less double beta decay experiments, if the scale is in the tens of meV range. The Feynman diagram is illustrated in Figure 10. The neutrino must be Majorana for this to proceed. The extremely small rates, and significant backgrounds from double-beta decay itself, push the detector requirements to unprecedented territory.

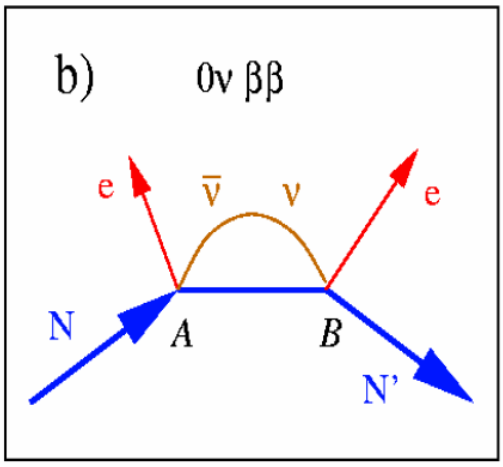

Figure 10. Feynman diagram for neutrino-less double beta decay.

4. SOME IMPORTANT TRENDS IN DETECTOR ADVANCES

Advances in detector technology, in many cases, derive from trends which can be systematically categorized. In the following few sections, a number of these trends are described. These trends are not completely independent.

4.1. Segmentation

One important trend has been the development of detector elements with increasingly smaller size. For example, vertex detector elements measuring 10 microns or less are now feasible. Advances in the micoelectronics industry has been important to this development. Calorimeters employing silicon enable fine segmentation of the sampling media. Bump bonding technology enables low capacitance connections. Modern etching technology has enabled the development of Micro Pattern Gas Detectors (MPGD)[15], revolutionizing cell size limits in many gas detector applications.

Granularity is often limited by trade-offs between read-out design, signal/noise ratio, and power considerations. The state-of-the-art in microelectronics or etching technology may set these limitations.

Several examples of proposed increases in granularity are given by envisioned ILC detector designs. The silicon-tungsten electromagnetic calorimeter might employ about 10^8 12 mm^2 cells.[16] The digital hadron calorimeter could employ half this number of one cm^2 cells.[17] A detector employing a Time Projection Chamber would deploy MPGDs for fine granularity readout, or even a silicon device (the Medipix2 chip is being studied in this context as a proof of principle.) As already referenced, the vertex detector would employ a billion pixels of less than 20 μm^3 volumes. Note the thin sensitive depth is of significant value in establishing a precise spacepoint.

4.2. Speed

Speed is usually a critical parameter in detectors. At the Super LHC, pile up of events will be a limiting issue. At the ILC the accumulation of background hits in the inner layer of the vertex detector is a major challenge. Similar issues must be faced at the Super B Factory.

Faster electronics, with low noise and low power, is a valuable trend. A notable advance in speed has also been achieved by the Micro Pattern Gas Detectors, the Micromegas and GEMs. They have produced good detection efficiency, with accuracy (< 100 μm), at high rates (nearly MHz mm^{-2}). Recent developments are reported at this conference.[18]

4.3. Growth and Integration

In their review paper of 1999,[19] W.K.H.Panofsky and M.Breidenbach noted the continuous growth over three decades in instrumented signal channels and data rate in major HEP experiments. Figure 11 is their illustration of this trend. They said "growth with only moderate cost increase rests largely on continuing developments in circuit integration and computing technologies." The growth trend continues, but microelectronics and mechanical sophistication has changed its character. High degrees of multiplexing is being deployed. For example, the 307 million pixels of the SLD vertex detector were read out through 384 channels. The ILC silicon-tungsten electromagnetic calorimeter design[16] reads 1024 pixels of the calorimeter through each readout channel. This means 100 million calorimeter cells require only 100,000 readout channels.

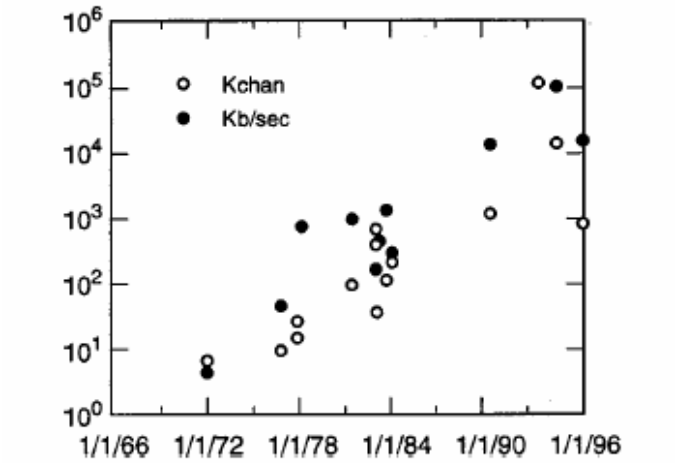

Figure 11. Evolution of the number of detector signal channels with time. Open circles: number of electronic instrumentation channels in thousands; closed circles: design data rate in kilobytes per second to permanent storage. See [19] for details.

4.4. Power constrained low noise electronics

It has been shown[20] that the principles applied to "highly segmented detectors" can be generalized. First, finer segmentation often does not reduce signal. However, noise is reduced due to lower capacitances, lower leakage currents, and lower rate/pixel. Figure 12 illustrates this trend.

Cost is weakly dependent on the number of pixels, being often dominated by total area.

Noise control demands the electronics be close to the active detector elements in order to minimize capacitances.

Temperature control is required to control leakage currents, and gain inhomogeneity. Therefore, practical power dissipation is a critical design issue

Front-end design choices for noise, shaping time, and power budgets need care.

Interconnect issues are of increasing importance with finer pixel size.

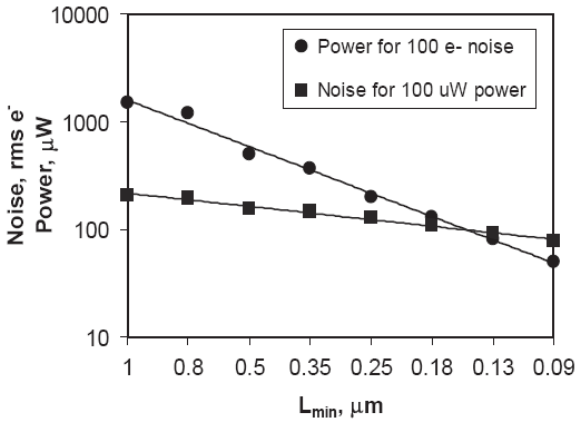

Figure 12. Power and noise evolution with technology generation for CMOS charge-sensitive preamplifiers with NMOS front end. Detector capacitance = 1 PF; peaking time = 50 ns.[20]

The semiconductor industry anticipates the future feature sizes in silicon technology, which is illustrated by the roadmap shown in Table 1.[21] Over the next decade, one can expect a three-fold feature size reduction, or a ten-fold transistor density increase.

	2004	2007	2010	2013	2016
Technology Node [nm]	90	65	45	32	22
Transistor count [Mtr]			1500	3092	6184
Transistor Density [Mtr/cm2]	77	154	309	617	1235
Chip Size	140				280
Clock freq [GHz]	3		15		53
Vdd	1.2	1.1	1.0	0.9	0.7
DRAM half pitch	90	65	54	32	22
Signal IO Pads	512	1024	1024	1024	1024
Power Pads	1024				2048

Table 1. International Technology Roadmap for Semiconductors, A. Marchioro, CERN-PH, 2005

4.5. Mechanical complexity

Advances on the mechanical technology leads today to detector designs which are highly radiation resistant, robust, thin, and durable. Careful and skilled mechanical design and construction optimizes detector performance. Modern detectors are compact, highly integrated, and thin, resulting in ultimate operation.

Developments for future experiments include a very thin silicon layer for the ILC vertex detector (illustrated by Figure 13), where ~ 0.1% X_0 per layer is envisioned, and the very dense silicon/tungsten electromagnetic calorimeter for the SiD experiment at the ILC, shown in Figure 14.

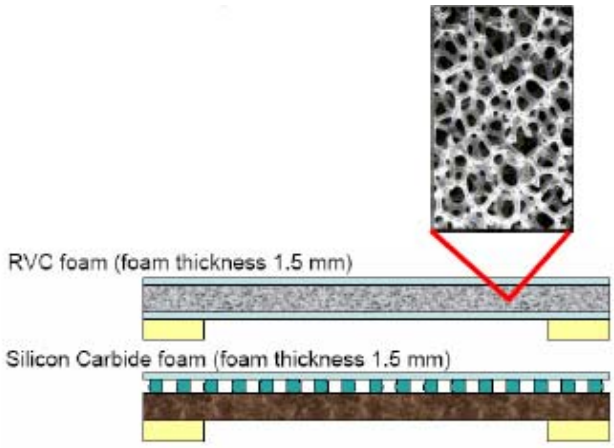

Figure 13. Illustration of low mass ladders under development by LCFI Collaboration.[38]

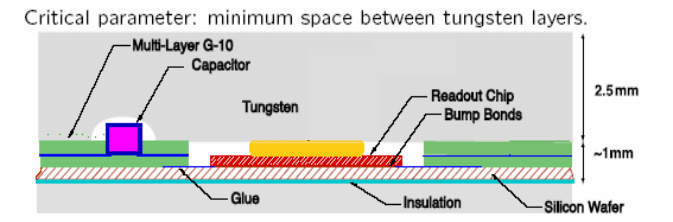

Figure 14. Schematic of the cross-section of the Si-W EM calorimeter layer, showing the embedded readout chip.[16]

4.6. Radiation Immunity

With accelerator technology advances producing higher luminosities, experiments are required to confront ever higher radiation exposures. Even moderate levels of radiation exposure will limit detector options.

The Super LHC tracking environment is the most hostile of the planned future experiments. 10^{16} neq/cm^2 are expected at 5 cm radius, 10^{15} neq/cm^2 at 20 cm radius, and 2×10^{14} neq/cm^2 at 50 cm radius.[22]

The forward, small angle detectors of the ILC must tolerate high doses, such as one GigaRad/year in the BeamCal.[23]

Several MRad per year are anticipated in the Super B Factory vertex detector.[24]

Recent advances in understanding damage mechanisms and annealing mechanisms have been critical to increased ability to deal with these very high dose rates. Several reports at this conference deal with such recent developments.[25]

5. EXAMPLES OF PLANNED AND PROPOSED FUTURE DETECTORS

5.1. Calorimetry

Detector R&D for future experiments is vigorous, and several examples are described below.

5.1.1. Digital Hadron Calorimetry

An effort within the CALICE Collaboration is developing the digital hadron calorimeter based on RPCs and GEMS for the ILC. A few layer test has started at Fermilab. The goal is to build up a one meter-cubed prototype to decisively test the concept. A lateral readout segmentation of one square centimeter is planned, with layer-by-layer longitudinal readout. This prototype is aimed at validating the RPC and GEM approach as an active element, to validate the electronics readout, to measure the hadronic showers with unprecedented resolution, to validate the Monte Carlo simulations of the hadronic showers, and to compare results with those from an analog scintillator hadron calorimeter.

5.1.2. Silicon/Tungsten Electromagnetic Calorimetry

A fine grained electromagnetic calorimeter serves several goals toward optimized physics performance of the ILC experiments. It is critical to the success of the particle flow technique for hadron jet calorimetry (see the next section), but also is important for other physics, such as the tau decay reconstruction illustrated by Figure 15.

A natural technology choice is the silicon-tungsten (SiW) sampling calorimeter.[26] Good success was achieved using SiW for luminosity monitors at SLD,[27] DELPHI,[28] OPAL,[29] and ALEPH.[30] SiW sampling calorimetry specifically optimized for the ILC experiments is under development.

The SLAC/Oregon/BNL/Davis/Annecy Collaboration is developing a very dense, fine grained silicon tungsten calorimeter for the ILC.[16] The pad size for this device (see Figure 16 for an early prototype) would be 12 mm^2 to match Moliere radius (~ $R_m/4$). Each six inch wafer of 1024 pads is read out by one integrated chip (KPiX). Tests have demonstrated that less than 1% crosstalk is expected. A KPiX design has been fabricated and is under test. In order to be sensitive to single minimum ionizing particles, the signal-to-noise must exceed seven, making the required noise level less than 2000 electons. A dynamically switchable feedback capacitor scheme achieves required dynamic range of 0.1-2500 MIPs. The mechanical design calls for passive cooling, with heat conducted in the tungsten to the edge of each module.

The CALICE Collaboration is also developing an ILC silicon-tungsten calorimeter, and has already collected initial test beam data with a prototype module, first at DESY, and then at CERN.

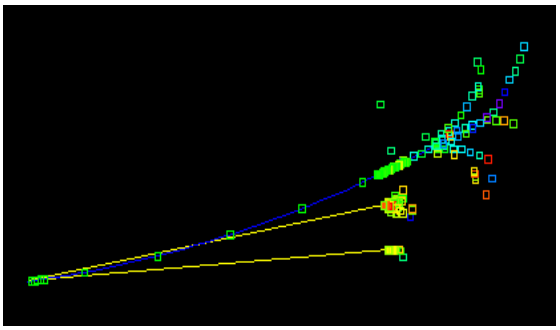

Figure 15. Simulated τ decay to $\rho\nu_\tau$, with the interaction of two γs from the π^0 decay, and the charged π in the highly pixelated calorimeter.

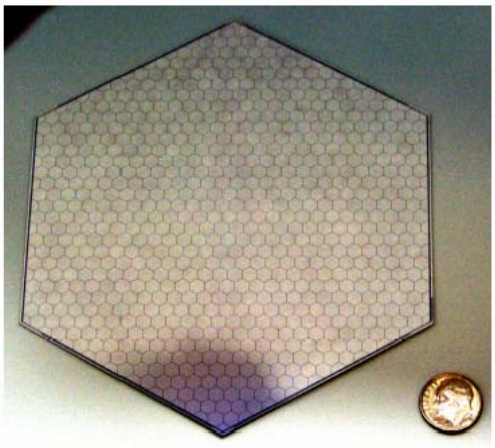

Figure 16. Prototype Si-W EM calorimeter wafer array.[16]

5.1.3. Particle Flow Calorimetry

The features of ILC events make particle flow calorimetry an attractive approach for optimal jet energy resolution. The typical distributions of charged and neutral hadron, and electromagnetic energy content of 100 GeV jets at the ILC is illustrated in

Figure 17.[31] Charged hadrons, which are measured by the inner tracker with far better resolution than can be achieved in a calorimeter, dominate the energy content. This motivates using the excellent resolution of the tracker, and adding the missing neutral elements with measurements in the calorimeter.

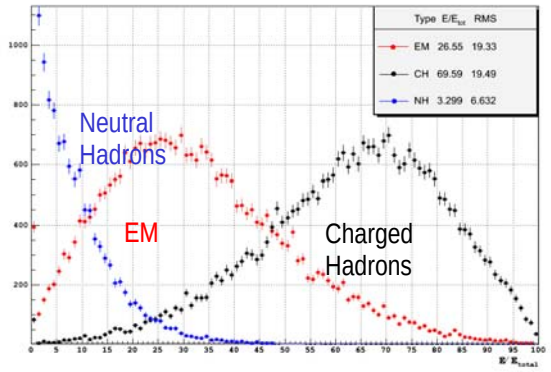

Figure 17. Distributions of energy fractions in high energy jets in $e^+e^- \rightarrow$ t anti-t at $\sqrt{s}$ = 500 GeV. Abscissa displays fraction from 0 to 100%. [31]

Table 2 summarizes the contributions of each component of the jet to the overall resolution. In the absence of confusion between components, using the tracker and calorimeter in this coordinated way, a resolution of about 20%/√ E is ideally possible. The goal of the current R&D program is to establish about 30%/√ E.

Particles in Jet	Fraction of Vis. Energy	Detector	Resolution
Charged	~65%	Tracker	< 0.005% p_T negligible
Photons	~25%	ECAL	~ 15% / √E
Neut. Had.	~10%	ECAL/HCAL	~ 60% / √E

Table 2

Such precision requires unprecedented granularity in order to separate the various components. As an example, the SiD detector concept being developed for the ILC foresees 90 million 12 square-millimeter cells in the silicon-tungsten electromagnetic calorimeter, and 40 million one square-centimeter cells in the digital hadron calorimeter.

Prototyping and beam tests are underway to establish this capability. Simulation studies have been encouraging. Figure 18 shows an event simulation in which the separation of individual components of a jet are seen, showing the feasibility of the approach when the calorimeter provides a high degree of segmentation. Several independent studies of jet reconstruction are in progress.

Figure 19 shows results from one study[32] of reconstructed jet energy resolution of the Z reconstruction for a detector operating at the Z, and reconstructing light quark events.

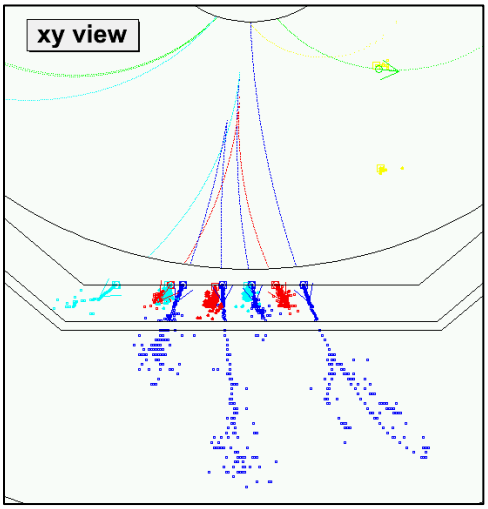

Figure 18. Simulation of jet interaction with calorimeter.[32]

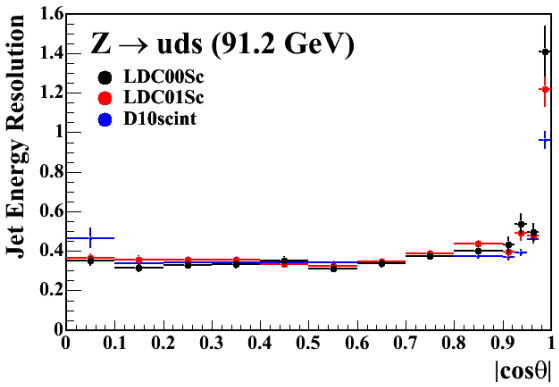

Figure 19. Jet energy resolution for particle flow reconstruction of light quark jets at the Z resonance.[32]

5.1.4. Dual Readout Calorimetry

One approach which has been proposed[33] to enable compensation between electromagnetic and hadronic components of hadronic showers is the separate readout of scintillation and Cherenkov signals within the hadron shower. Since these two signals have different sensitivities to electromagnetic and hadronic components of a hadronic shower, one can then, in principle, establish compensating calorimetry in analysis. This idea has been realized now by the Dream detector, consisting of scintillator and quartz fibers.[34]

Figure 20 presents a result from this calorimeter in which the individual scintillator and quartz responses are shown, along with the optimized combination of the two, which achieves improved resolution. Ideal application of this technique to an experiment is challenging due to the limited transverse and longitudinal segmentation.

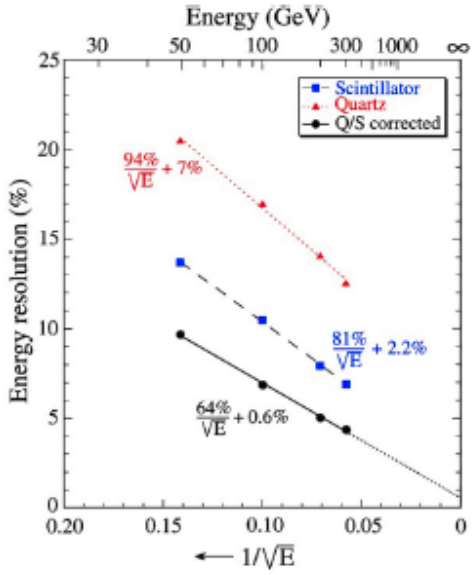

Figure 20. The jet energy resolution as a function of energy, measured with scintillation fibers, Cherenkov fibers, and after corrections, from the dual readout calorimeter described in [34].

5.1.5. Rad-hard Crystals

Progress continues on the development of radiation hardened crystals for electromagnetic calorimetry. The endcap radiation damage for CMS crystals at SLHC is unacceptable. An attractive prospect to replace the lead tungstate crystals is[35] LSO/LYSO (Ce:Lu_2SiO_5, Cerium doped Lutetium Orthosilicate; $Lu_{2(1-x)}Y_{2x}SiO_5$: Ce - Cerium doped Lutetium Yttrium Orthosilicate). This crystal is expected to produce a better energy resolution at low energy than the L3 BGO or CMS PbWO crystals, because of its high light output and low readout noise. It has a less stringent environment due to its small temperature coefficient. And it is more rad hard than PbWO. The proponents are also investigating its application to the Super B Factory and the ILC.

5.2. Silicon Tracking

Silicon tracking detectors are used for the inner vertex detector trackers, as well as the outer tracking in a number of experiments today, and proposed future experiments.

5.2.1. Advanced pixels for Super LHC

As already described above, the fluence of tracks within a radius of 20 cm at the SLHC is so intense (> 10^{15} /cm^2) that a new technology is required to deal with it. Figure 21 illustrates this challenge.[36] 50 μm × 50 μm pixel size is required in this region, and the signal over threshold must be held about five throughout the lifetime of the sensor. Several possible solutions are under development, including CVD diamond,[37] monolithic pixels, cryogenic silicon, and 3D detectors. Figure 22 illustrates the geometry of the 3D detectors, which achieve increased electric fields, and shortened collection distances, thereby promising improved radiation tolerance. Etched holes as deep as several hundred mirons are separated by as little as 50 microns.

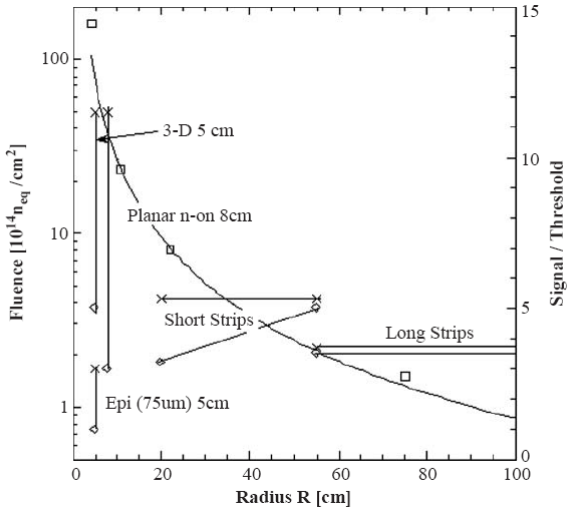

Figure 21. The fluence for an integrated luminosity of 2500 fb^{-1} as a function of radius R (left scale) is based on the data of open squares, with a fit of the form 1150/R$^{1.6}$ superposed. The anticipated signal-to-threshold ratios (right scale) for silicon detectors in the tracker regions with the initial value (x) and that after an integrated luminosity of 2500 fb_1 (diamond).[22]

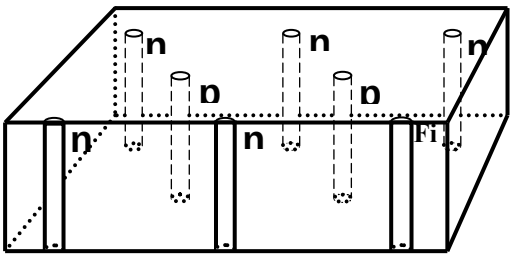

Figure 22. 3D detector geometry.

5.2.2. ILC Inner Tracking/Vertex Detection

The ILC environment offers a unique environment in which to achieve exceptional physics goals, due to the modest event rates, relative rates of background to signal, and relatively low radiation levels. Precision measurements of the branching ratios for many of the Higgs decay modes is a primary goal, and superb flavor tagging is needed to achieve this. The goal for the impact parameter resolution is 5μm ⊕ 10μm/(p sin$^{3/2}$θ). Excellent spacepoint precision of better than 4 microns is needed. The transparency requirement on each layer of the vertex detector is ~0.1% X_0. The spacepoint precision of 3.9

microns and transparency of 0.4% X_0 achieved by SLD encourages this. Track reconstruction within the vertex detector alone is planned, based on a five barrel pixel detector.

Several concepts are under development to achieve these ILC vertex detector performance parameters. The operating environment of the ILC, with bunch trains of about 3000 bunches, each pair separated by about 300 nanoseconds, is a demanding constraint on the design. The concepts under active development include Charge-Coupled Devices (CCDs), CPCCD (column parallel CCDs), monolithic active pixels based on CMOS technology, DEPFETs (DEpleted P-channel Field Effect Transistor), SoI (Silicon on Insulator), ISIS (Image Sensor with In-Situ Storage), and Hybrid Active Pixel Sensors (HAPS).

5.2.3. Column Parallel Readout CCDs

The SLD vertex detector[11] was designed to read out 800 kpixels/channel at 10 MHz, and was operated at 5 MHz. That is, the readout time was 200 msec/channel. With the time structure of the ILC, much faster readout is required. A possible solution for CCDs is the column parallel readout (CPCCD) approach. The Linear Collider Flavor Identification (LCFI) Collaboration has pioneered this approach.[38] A separate amplifier and readout is provided for each column of the CCD. (See Figure 23.) This results in an increased speed factor of several hundred.

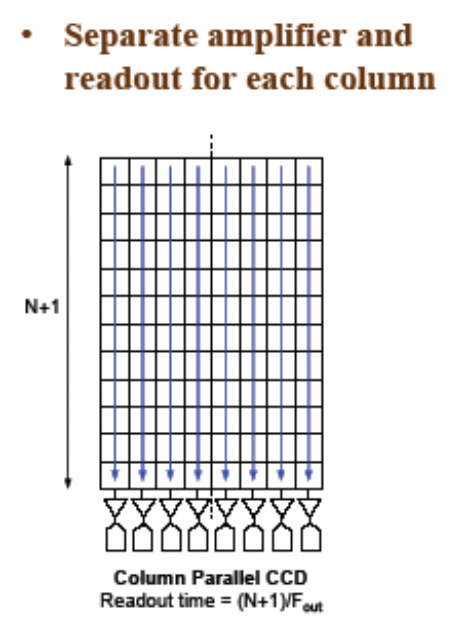

Figure 23. Illustration of a column parallel CCD.[38]

The first generation tests of the CPCCD prototypes yielded 100 electron noise (reduced to 60 with filtering), minimum clock potential of about 1.9 volts, and a maximum clock frequency of better than 25 MHz. A second generation is under test, with three different image areas: 92 mm x 15 mm, 53 mm long, and13 mm long.

5.2.4. ISIS

The intense, very short bunches of the ILC create a concern for electromagnetic interference (EMI), particularly for active elements in the vertex detector. SLD delayed operation of the vertex detector readout during beam passage in response to beam related interference. The Image Sensor with In-situ Storage (ISIS)[39] offers robust storage of charge in a buried channel during beam passage. The technique has been used up to a speed of 1 Megaframe/second.

The ISIS sensor for the ILC provides CCD-like charge storage cells in CMOS or CCD technology, processed on a sensitive epi layer. A p+ shielding implant forms a reflective barrier (deep implant). A test device has been built by e2v and is being evaluated by the LCFI Collaboration.

5.2.5. DEPFETs

The DEPFET (DEpleted P-channel Field Effect Transistor) device is illustrated in Figure 24.[40] A field effect transistor sits on fully depleted bulk. All charge generated in the bulk collects beneath the transistor channel, steering the transistor current. The charge can be cleared by a positive pulse on the clear electrode. The net effect is a combined sensor and amplifier.

The attractive features of the DEPFET are: 1.) low capacitance, yielding low noise, 2.) signal charge undisturbed by readout, permitting repeated readout, 3.) complete clearing of signal charge, meaning no reset noise, 4.) sensitivity over full depth of bulk, yielding large signals for mips, 5.) charge collected during off mode, resulting in low power consumption, 6.) measurement at place of generation resulting in no charge transfer loss, and 7.) operation over very large temperature range, with no cooling needed.

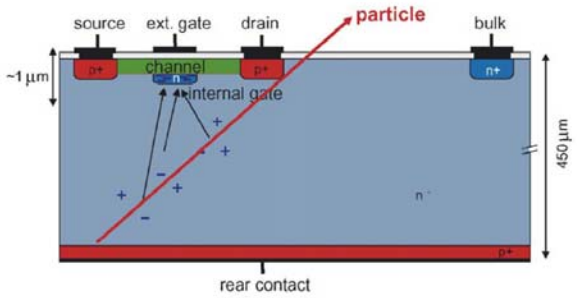

Figure 24. Cross-section of a DEPFET pixel through the transistor channel,illustrating the principle of operation.[40]

5.2.6. Monolithic CMOS

Monolithic CMOS sensors have been developed from the standard VLSI chip, with a thin, un-doped silicon sensitive layer, operated undepleted. It decouples charge sensing and signal transfer, leading to improved radiation tolerance and random access. Very fine pitch is feasible, resulting in high tracking precision. The devices are thin, fast, and of moderate cost.

Strasbourg IReS has been working on development of monolithic active pixels since 1999; other groups are also actively developing variants (eg. RAL, Yale/Oregon., etc.) The initial IReS prototype arrays containing a few thousands pixels demonstrated the viability of the concept. Large prototypes have now been fabricated and tested.[41]

Recent attention has been addressing readout strategies adapted to specific experimental conditions, and transfer of the technology to AMS 0.35 OPTO from TSMC 0.25, aiming for increased epi-layer thickness (~12 μm vs. < 7 μm.) The devices are being applied to the STAR detector.

Several parallel CMOS efforts include the FAPS (Flexible Active Pixels) which integrate 10-20 storage capacitors per pixel,[42] the Chronopixel concept which time stamps hits with single bunch precision,[43] as well as others.

5.2.7. ILC Silicon Tracking

A silicon microstrip tracker is being developed for the ILC. A key aspect of the design is the very thin modules, achieving about 0.8% X_o per layer in the central barrel. The tracker is incorporated with a pixel vertex detector for track finding. This approach (advocated by the SiD concept[17]) is motivated to manage the increased radiation and pile-up expected to accumulate over the long bunch trains of the ILC. The fast response of silicon is immune to this. Superb spacepoint precision of silicon allows tracking measurement goals to be achieved in a compact tracking volume. The tracker is robust to spurious, intermittent backgrounds. The compactness of the tracking system allows for more aggressive technical choices for outer systems (assuming an overall cost constraint). The third dimension is "measured" and backgrounds are suppressed by segmented silicon strips. Figure 25 illustrates the resolution that might be achieved, depending on the thickness and resulting multiple scattering of the silicon layers (SD Thin or SD Thick.)[44] SiD would approach SD Thin with its thin modules.

5.3. ILC TPC Tracking

Complementary to silicon tracking, another approach being developed for the ILC is based on Time Projection Chamber technology. This builds on the successful experience of many experiments, including PEP-4, ALEPH, ALICE, DELPHI, and STAR.

The large number of space points makes reconstruction straight-forward, assuming tolerable confusion from backgrounds. The dE/dx measurements provide a bonus of particle ID. The minimal material in the tracking volume is helpful for barrel calorimetry. Tracking extends to large radii. New readout designs under development promise to improve robustness and precision.

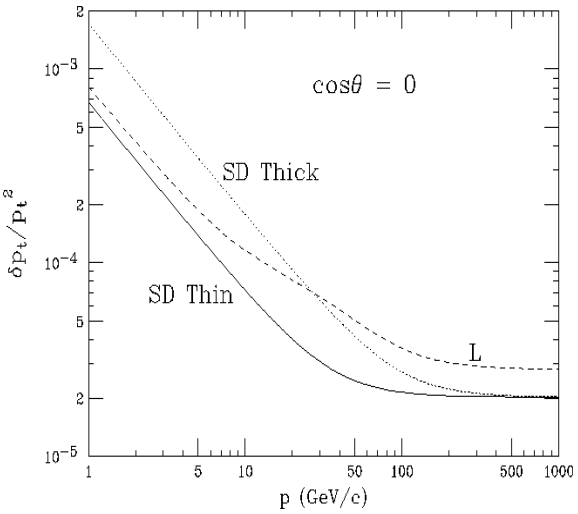

Figure 25. Momentum resolution of two extremes of a compact silicon tracking system for the ILC, labelled SD Thick and SD Thin in reference to the amount of material in the tracker. For comparison, the resolution of a larger gaseous tracker (L) is shown.[44]

A very active R&D effort for the ILC is addressing a number of technical issues.[45] These include optimizing the novel gas amplification systems. The conventional TPC readout, based on MWPC and pads, is limited by positive ion feedback and MWPC response. This can be improved by replacing the MWPC readout with micropattern gas chambers (GEMs or Micromegas). Such chambers provide small structures (eliminating E×B effects), have 2D profiles, limit signals to that of the fast electrons, and offer intrinsic ion feedback suppression

Other issues to be addressed are the neutron backgrounds, optimization of single point and double track resolution, performance in high magnetic fields, demonstration of large system performance with control of systematics, and endplate design for minimal material.

Figure 26 and Figure 27 illustrate the GEM towers employed by COMPASS: double sided, copper coated, 50 μm kapton foil, with 75 μm holes on a 140 μm pitch. The GEM voltages range up to 500 V, and yield a gas amplification of 10^4.

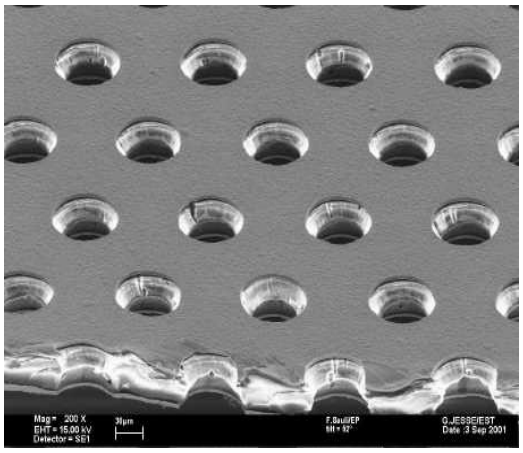

Figure 26. Electron microscope picture of a GEM foil, with 70 μm diameter holes, on a 140 μm pitch.[46]

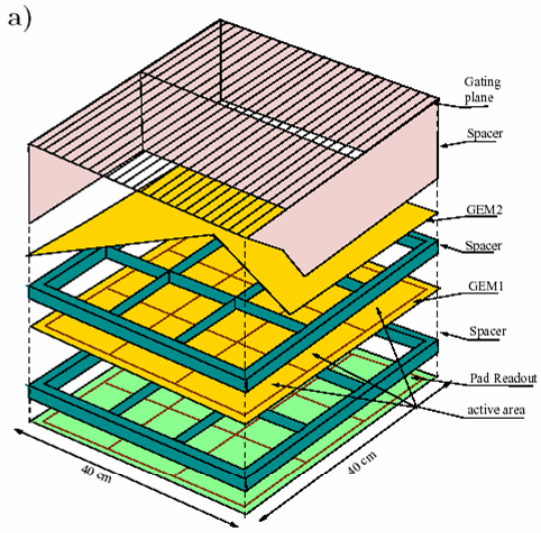

Figure 27. Schematic of GEM detector.

An application of Micromegas for the TPC readout is illustrated with Figure 28. An asymmetric parallel plate chamber with micromesh is used, resulting in saturation of the Townsend coefficient, and a mild dependence of amplification on gap variations. Ion feedback is suppressed.

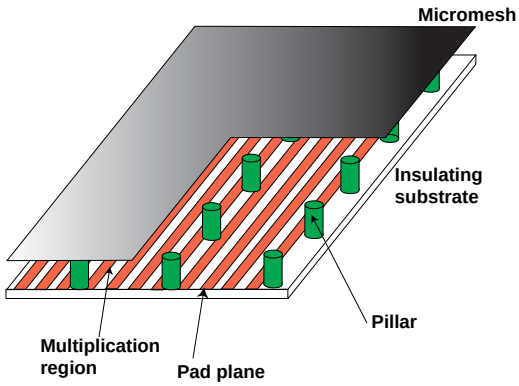

Figure 28. Illustration of the Micromega mesh used for a TPC readout.

Application of silicon (Medipix2) w/ GEMs for the TPC readout is also an active area of investigation.[47]

5.4. Cherenkov Detectors

Ring imaging detectors have provided a powerful tool for recent and present experiments, such as the CRID of SLD, the RICH of DELPHI, and the DIRC of BaBar. Cherenkov radiation will continue to be an important detector tool in the future. It is used in dual readout calorimetry, as already mentioned. It is being developed to detect and measure high energy neutrino interactions.[48] Applications of thick GEMs to the ring imaging technology[49] promises to advance the particle ID technology. Finally, aerogel radiator continues to play a useful role in this area.[50]

5.5. Neutrino Detectors

Neutrino physics has benefited in recent years from significant advances, and detector technology is critical to future advances. Two particularly interesting areas of development are the liquid argon TPC detector, and the liquid noble element detector designed for neutrino-less double beta decay detection. Likewise, high spatial resolution calorimeters are being developed using liquid noble elements for other applications.[51]

Figure 29 shows a hadronic interaction image from the Icarus liquid argon TPC detector. The ICARUS detector[52] consists of number cryostats, each filled with about 300 tons of liquid Argon (LAr) and equipped with a novel drift chamber operated in very high purity LAr. A 300 ton calorimeter has been in operation for several years.

Figure 29. Hadronic interaction in ICARUS.[52]

The EXO (Enriched Xenon Observatory) Collaboration is developing a 10 ton detector for neutrino-less double beta decay, with sensitivity for Majorana neutrino masses of about 0.01 eV. The highly (80%) enriched (isotope 136) Xenon yields a barium atom upon decay, which is then detected via high resolution, single atom spectroscopy. 200 kg of highly enriched Xenon has been accumulated, and preparations are underway for an underground test.[53]

6. CONCLUSION

Physics opportunities for the next decade are fundamental to our understanding of the Nature of the Universe ("the Quantum Universe"). Experimental opportunities following current experiments, including upgrades as well as new colliders, should be excellent. These opportunities bring new and difficult challenges to the experimenter. Trends in the advances of detector technology promise to provide continued progress in addressing the challenges. At this conference we will hear the latest progress on many important developments, and their connections to other fields from experts in detectors.

Acknowledgments

The author thanks the SNIC06 organizers for the invitation to present this talk. He also thanks colleagues for critically reading and commenting on this paper, including M. Breidenbach, C.J.S.Damerell, R. Heuer, J. Jaros, R. Frey, R. Settles, and D. Strom.

Work supported by grants from the Office of Science of the U.S. Department of Energy, and the National Science Foundation.

References

[1] R. Gaitskell, this symposium.
[2] LEP Electroweak Working Group, hep-ex/511027 (2005).
[3] The ALEPH, DELPHI, L3, OPAL, SLD Collaborations, the LEP Electroweak Working Group, the SLD Electroweak and Heavy Flavour Groups, "Precision Electroweak Measurements on the Z Resonance," Phys.Rept. 427 (2006) 257.
[4] W.-M. Yao et al., J. Phys. G 33, 1 (2006); http://pdg.lbl.gov/2006/reviews/kmmixrpp.pdf.
[5] http://hitoshi.berkeley.edu/neutrino
[6] F. Gianotti et al., Eur.Phys.J. C33 (2004) 273-296.
[7] U. Baur, T. Plehn, and D.L. Rainwater, Phys.Rev. D67 (2003) 033003.
[8] S. Tapprogge, ATLAS Week, February, 2005.
[9] P. Nevski, ATLAS Week, February, 2005.
[10] S. Yamashita, 7th ACFA Workshop, Taipei, 2004.
[11] K. Abe et al., Nucl. Inst. and Methods A400, 287, 1997.
[12] A. G. Akeroyd , "Physics at Super B Factory," hep-ex/0406071
[13] D. Hitlin, Super B Factory Workshop, January, 2004.
[14] M. Lindner, 3rd ICFA Seminar, Daegu, September, 2005.
[15] Y. Giomataris, Nucl. Inst. and Methods A376, 29 (1996); F. Sauli, Nucl. Inst. and Methods A386, 531 (1997).
[16] D. Strom et al., 2005 International Linear Collider Workshop, Stanford, 2005.
[17] J. Brau, M. Breidenbach, and Y. Fujii, SLAC-PUB-11413, 2004.
[18] I. Giomataris (Saclay), High Rate Capability of Micromegas; Fabio Sauli, Recent developments in Micro-Pattern Gas
[19] W.K.H. Panofsky and M. Breidenbach, "Accelerators and detectors," Rev. Modern Physics 71, S121 (1999).
[20] P. O'Connor, NIM A522, 126 (2004)
[21] A. Marchioro, CERN-PH, 2005; International Technology Roadmap for Semiconductors, public.itrs.net.
[22] H. Sadrozinski, A 552 (2005) 1.
[23] W. Lohmann, private communication.
[24] T. Iijima, Super B Meeting, Frascati, November, 2005.
[25] M. Bruzzi, M. Swarz, R-Y. Zhu, V. Lepeltier, J. Schwiening, presentations at this symposium.
[26] J.E. Brau, A.A. Arodzero, and D.M. Strom, Proceedings of the 1996 DPF/DPB Summer Study on High Energy Physics, 437 (1997); http://www.slac.stanford.edu/pubs/snowmass96/PDF/DET077.PDF.
[27] S. Berridge et al., IEEE Trans. Nucl. Sci. 37, 1191 (1990) ; S. Berridge et al., IEEE Trans. Nucl. Sci. 39, 1242 (1992).
[28] S. Almehed et al., Nucl. Inst. and Methods.A305, 320, (1991).
[29] G. Abbiendi et al., Eur. Phys. J. C14, 373 (2000).
[30] D. Bederede et al., Nucl. Inst. and Methods A365, 117 (1995).
[31] J. Yu, ALCPG Workshop, SLAC, 2004.
[32] M. Thomson, Linear Collider Workshop, Bangalore, 2006.
[33] D. R. Winn and W. Worstell, IEEE Trans. Nuclear Science Vol. NS-36 , No. 1, 334 (1989)
[34] N. Akchurin et al., Nucl. Instr. and Meth. A537 (2005) 537–561.
[35] R. Zhu, private communication.
[36] H. Sadrozinski, Nucl. Inst. and Methods A552, 1 (2005).
[37] W. Adam et al., Nucl. Inst. and Methods A565, 278 (2006).
[38] http://hepwww.rl.ac.uk/lcfi/
[39] W F Kosonocky et al IEEE SSCC 1996, Digest of Technical Papers, 182
[40] M. Trimpl et al., Nucl. Inst. and Methods A560, 21 (2006).
[41] G. Deptuch et al., Nucl. Inst. and Methods, A511, 240 (2003).
[42] J. Velthuis, Nucl. Inst. and Methods A560, 40 (2006).
[43] C. Baltay, this symposium.
[44] B. Schumm, private communication.
[45] http://www.mppmu.mpg.de/~settles/tpc/welcome3.html
[46] C. Altunbas et al., Nucl. Inst. and Methods A490, 177 (2002).
[47] P. Colas, Nucl. Inst. and Methods A535 506 (2004).
[48] G. Varner, this symposium.
[49] R. Chechik et al., Nucl. Inst. and Methods A553, 35 (2005).
[50] E. Kravchenko , this symposium.
[51] S. Peleganchuk, this symposium.
[52] S. Amerio et al., Nucl. Inst. Meth., A527 (2004) 329-410.
[53] http://www-project.slac.stanford.edu/exo/talks.html